IOP Publishing Superconductor Science and Technology
Supercond. Sci. Technol. **23** (2010) 025012 (6pp) doi:10.1088/0953-2048/23/2/025012

# Anisotropic transport properties in tilted *c*-axis $MgB_2$ thin films

**P Orgiani[1,2], Ke Chen[2,10], Yi Cui[2], Qi Li[2], V Ferrando[2,3], M Putti[3,4], M Iavarone[5], R Di Capua[6,7], R Ciancio[8], R Vaglio[7], L Maritato[1] and X X Xi[2,9,10]**

[1] CNR-INFM Coherentia and Department of Mathematics and Informatics, University of Salerno, I-84081 Baronissi (SA), Italy
[2] Department of Physics, Pennsylvania State University, University Park, PA 16802, USA
[3] CNR-INFM-LAMIA and Department of Physics, University of Genova, I-16146 Genova, Italy
[4] Applied Superconductivity Center, National High Magnetic Field Laboratory, Florida State University, Tallahassee, FL 32310, USA
[5] Materials Science Division, Argonne National Laboratory, Argonne, IL 60439, USA
[6] Health Sciences Department (S.pe.S), University of Molise, I-86100 Campobasso, Italy
[7] CNR-INFM Coherentia and Department of Physics, University of Napoli, I-80125 Napoli, Italy
[8] CNR-INFM National Laboratory TASC, I-84081 Basovizza (TS), Italy
[9] Department of Materials Science and Engineering, Pennsylvania State University, University Park, PA 16802, USA

Received 1 September 2009, in final form 16 October 2009
Published 18 December 2009
Online at stacks.iop.org/SUST/23/025012

**Abstract**
We report on superconducting magnesium diboride $MgB_2$ thin films grown on both YSZ and MgO substrates, with two different orientations, namely [110] and [211]. $MgB_2$ off-axis growth mode (namely, with the *c*-axis tilted with respect to the film surface's normal) is achievable on these substrates. Depending on the type and orientation of the substrate, tilting angle can be varied. As a consequence of tilted growth, anisotropic transport properties are observed. In very thin films, resistance measurements provide an estimate of the resistivity anisotropic ratio $\rho_c/\rho_{ab}$, where $\rho_c$ is the resistivity along the *c* axis and $\rho_{ab}$ is the in-plane resistivity. All these findings clearly demonstrate that tilted $MgB_2$ films offer new exciting possibilities to both investigate intrinsic fundamental properties of $MgB_2$ and to explore possible applications in planar superconducting devices.

(Some figures in this article are in colour only in the electronic version)

## 1. Introduction

After a few years on from the discovery of superconductivity in magnesium diboride $MgB_2$, the research activity on this material is still extremely high [1, 2]. The potential to scale superconducting electronics operating at relatively high temperatures and the fundamental physics of multi-gap nature of the superconductivity in $MgB_2$ have been giving a great impulse to the research on this material. Structurally, magnesium diboride consists of a layered structure of hexagonal honeycomb planes of boron atoms separated by planes of magnesium atoms. Indeed, two different gaps exist at $\Delta_\pi \sim 2.3$ meV and $\Delta_\sigma \sim 6.9$ meV, related to $\pi$ and $\sigma$ weakly interacting bands, respectively. Several experiments proved that the $\sigma$-carriers have negligible out-of-plane momenta, resulting in a substantial two-dimensional superconducting state, confined in the *ab* planes. Only carriers from the $\pi$-band have substantial momenta in the *c*-axis direction. Superconductor-based circuitry speed is ultimately limited by the energy gap of the superconductor. In this respect, it would be preferable to make $MgB_2$-based devices working with the larger gap. In fact, in

[10] Present address: Department of Physics, Temple University, Philadelphia, PA 19122, USA.

 

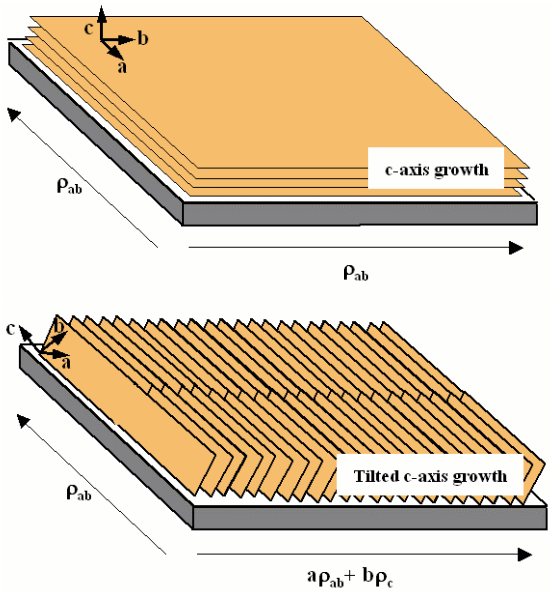


**Figure 1.** A schematic representation of the $MgB_2$ *c*-axis (upper panel) and tilted off-axis (lower panel) growth mode. Planes represent the boron/magnesium planes in the $MgB_2$ structure. The expected inequivalent resistivity path along the two in-plane crystallographic directions is also sketched.

sandwich-type Josephson junctions with *c*-axis $MgB_2$ films as the electrodes (figure 1(a)), only the smaller gap would be used [3, 4]. This difficulty can be overcome by choosing suitable substrates [5, 6], particularly those on which *c*-axis tilted films can grow as shown in figure 1(b). Tilted *c*-axis $MgB_2$ films were successfully grown on (110) yttrium-stabilized zirconium (YSZ) substrates. Scanning tunneling spectroscopy investigations of such samples have shown that the features representative of the sigma gap are present on the majority of the sample's surface [6], thus consistent with the tunneling current being injected into Mg/B *ab* planes.

Similar to the gap values, other physical properties (such as the critical current density and the critical field [7], the London penetration depth [8] and the resistivity [9]) were found to be anisotropic. In particular, to investigate the anisotropy in the transport properties, *c*-axis tilted $MgB_2$ films can provide an alternative method to evaluate the in-plane resistivity $\rho_{ab}$ (namely, resistivity within the Mg/B planes) and the out-of-plane resistivity $\rho_c$ (namely, the resistivity through the Mg/B planes). In tilted *c*-axis $MgB_2$ films, the two in-plane crystallographic directions are no longer equivalent, as happens in the *c*-axis $MgB_2$ film (see the schematic representation in figure 1). Keeping in mind the $MgB_2$ layered structures, in tilted films, the current could entirely flow along only the *ab* planes ($\rho_{ab}$), while in the orthogonal direction, the current flows through the different Mg/B planes by mixing the transport properties of the *ab* plane and the *c* axis ($a\rho_{ab} + b\rho_c$). By changing the tilting angle of the *ab* plane with respect to the film surface's normal, it would be possible to tune the contribution of the in-plane $\rho_{ab}$ and the out-of-plane $\rho_c$ resistivities to the total resistivity $\rho$, by ranging from the two extreme cases of $\rho = \rho_{ab}$ (namely, the *c*-axis-oriented film) and $\rho = \rho_c$ (namely, the *a*-axis-oriented film).

Depending on the specific choice of the substrate, $MgB_2$ thin films can be grown epitaxially, randomly oriented, *c*-axis-oriented and with the *c*-axis tilted away from the film normal [10]. The aim of this paper is to show that the tilted $MgB_2$ thin films are indeed achievable by choosing a suitable substrate. Moreover, the tilting angle can be varied by changing the specific type and orientation of the substrates. As a consequence of the tilted growth mode, an in-plane anisotropy in the transport properties of the films can be observed. Such a behavior can be ascribed to the specific film morphology, in terms of not-equivalent resistive paths, and to the anisotropic values of the out-of-plane $\rho_c$ and in-plane $\rho_{ab}$ resistivities. The presented results demonstrate new avenues to both probe intrinsic fundamental properties of $MgB_2$ and to explore new applications in superconducting devices.

## 2. Thin film growth and morphology

$MgB_2$ thin films were grown on YSZ and magnesium oxide (MgO) substrates, both with two different orientations, namely [110] and [211] by the hybrid physical chemical vapor deposition (HPCVD) technique. Detailed descriptions of the epitaxial growth of $MgB_2$ by HPCVD have been reported elsewhere [11]. $MgB_2$ has a hexagonal lattice structure ($P6/mmm$ symmetry space group), with in-plane and out-of-plane lattice parameters of 3.085 Å and 3.523 Å, respectively. YSZ has a cubic structure, with cell parameters which can slightly change due to the yttrium content. All the $MgB_2$ films presented in this work were grown on $Y_{0.18}Zr_{0.82}O_2$, which has a cell lattice constant of 5.16 Å. MgO also has a cubic structure, with a lattice constant of 4.217 Å. The tilted growth of $MgB_2$ films on all the substrates was primarily checked by scanning electron microscopy (SEM) analysis. The images of four 1500 Å thick $MgB_2$ films grown on (110)YSZ, (110)MgO, (211)YSZ and (211)MgO substrates are reported in figure 2. These films were grown during the same run by placing the four different substrates into the HPCVD system and the film thickness was measured by a standard profilometer on another $MgB_2$ film, grown during the same run.

SEM morphological studies show that $MgB_2$ films are formed by hexagonal grains of $MgB_2$ with their *c* axis away from the substrate normal. In the case of [110] orientation, for both $MgB_2$ samples grown on YSZ and MgO substrates, the in-plane rectangular symmetry of both substrates affects the growth mode of $MgB_2$ films, resulting in a mirror symmetry along one of the in-plane crystallographic axes. Such a degeneracy is not present in $MgB_2$ films grown on [211]-oriented YSZ and MgO substrates. In particular, for (211)MgO substrate, the $MgB_2$ planes are coherently oriented, piled on top of each other [5]. However, in the case of $MgB_2$ films grown on (211)YSZ substrates, a morphological arrangement similar to that found in both (110)YSZ/$MgB_2$ and (110)MgO/$MgB_2$ samples was observed, with a minor presence of *a*-axis (namely, *ab* plane normal to the film surface) grains.

X-ray diffraction analysis of the samples also confirm the existence of $MgB_2$ grains with different tilting angles. In the case of (110)YSZ/$MgB_2$, the $MgB_2$ *c* axis forms an angle of

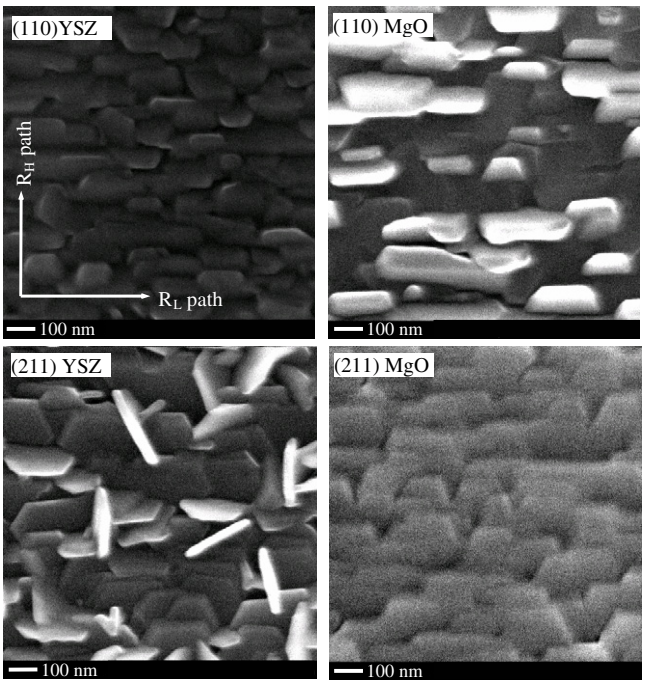


**Figure 2.** SEM images of four $MgB_2$ films grown on (110)YSZ, (110)MgO, (211)YSZ and (211)MgO substrates. In particular, on the SEM image of the film grown on the (110)YSZ substrate, the low-resistance ($R_L$) and the high-resistance ($R_H$) configurations are also sketched. The white arrows refer to the two directions of the measurement current, respectively.

32° with the normal to the substrate surface, while $MgB_2$ films grown on (112)YSZ do not show a unique crystallographic orientation, thus confirming the morphological analysis by SEM. In $MgB_2$ films grown on MgO substrates, such a tilting angle was found to be about 20° and 41° for [211] and [110] MgO orientations, respectively. $MgB_2$ films grown on YSZ substrates proved to be the most stable when exposed to the air, thus making possible a clearer understanding of the transport properties in terms of intrinsic (anisotropic resistivities) rather than extrinsic (degradation, precipitates, etc) phenomena at play.

Thin film morphology was also investigated as a function of the film thickness. In particular, atomic force microscopy (AFM) investigation was carried out on $MgB_2$ films (with different thicknesses) grown on (110) YSZ substrates. AFM experiments performed on 600 Å (figure 3(a)) and 3000 Å (figure 3(b)) thick $MgB_2$ films grown on (110)YSZ substrates are reported in figure 3.

For the thinnest films, the AFM image clearly shows the $MgB_2$ growth in the form of elongated island-type grains with in-plane dimensions of 200 × 60 $nm^2$. Such an overall in-plane orientation of the $MgB_2$ grains is representative of the whole film (up to millimeter scale), thus confirming the SEM results obtained on a 1500 Å thick $MgB_2$ film (figure 2). For thicker films (3000 Å), the AFM images show that the grain size is larger and they lose their preferential growth direction which turns into an in-plane randomly oriented grain growth. From these data, it is clear that the tilted growth mode only survives for thin films and, by increasing the film thickness, the preferential order of the tilted $MgB_2$ grains is reduced.

## 3. Transport properties

Electrical transport measurements were carried out by a standard four-probe dc technique. Since $MgB_2$ is easily degraded by water [12], which may be inevitably encountered during photolithography, all the transport properties reported here were measured on unpatterned films. All the films were deposited on 5 × 5 $mm^2$ square-shaped substrates, diced by a diamond blade along the in-plane crystallographic direction. Transport properties in $MgB_2$ tilted films have been investigated by standard Van der Pauw (VDP) configurations [13], by making the current flow along the two in-plane crystallographic axis of the film/substrate (see figure 1). The VDP configuration is a powerful way to detect both inhomogeneities (in particular for superconducting samples [14]) and anisotropies in the resistive paths [15]. Figure 4 shows the resistance versus temperature behavior for the same set of four 1500 Å thick $MgB_2$ films grown on [110]- and [211]-oriented YSZ and MgO squared substrates as used in figure 2.

All the $MgB_2$ samples show anisotropic behavior of the resistance, depending on the two VDP configurations. It is remarkable that, for all samples, both configurations show a sharp superconducting transition at about 39 K,

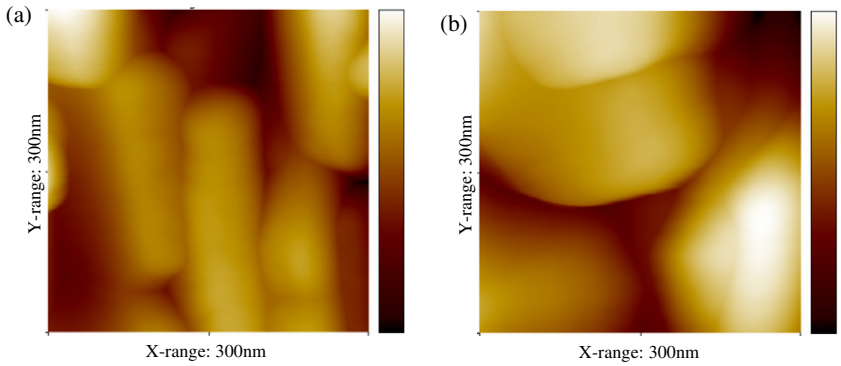


**Figure 3.** Atomic force microscopy experiments performed on 600 Å (a) and 3000 Å (b) thick $MgB_2$ films grown on (110)YSZ substrates. Data refer to a 300 × 300 $nm^2$ area.

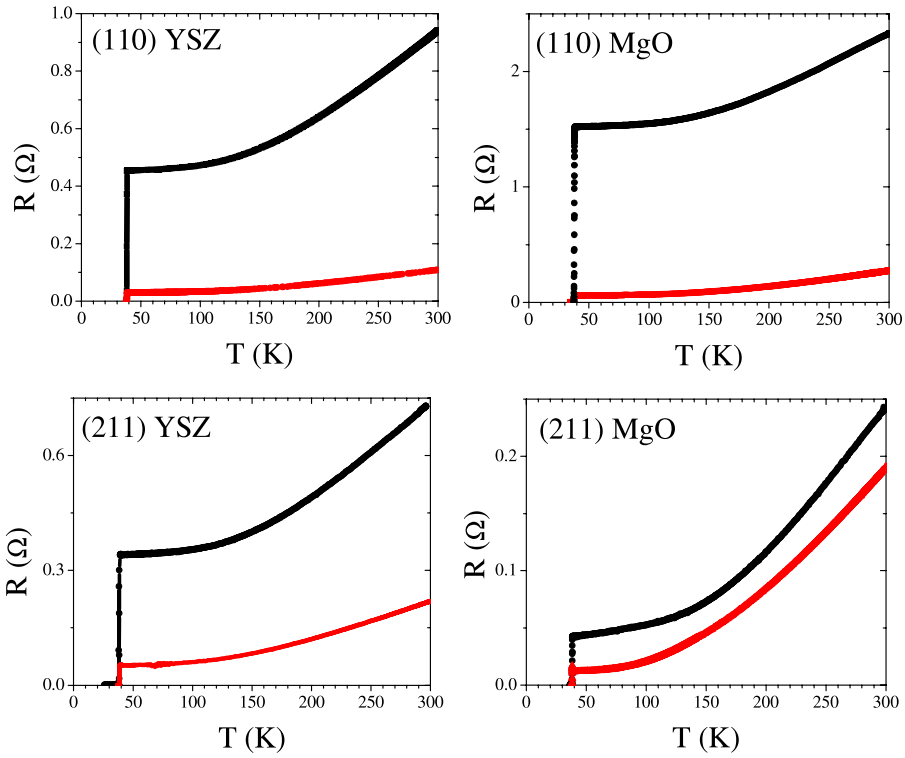


**Figure 4.** Resistance versus temperature behavior of 1500 Å thick $MgB_2$ films. Red curves refer to low-resistance path (current flowing in the $R_L$ direction in figure 2), corresponding to the $\rho = \rho_{ab}$ geometry (see sketch in figure 1, on the SEM image of $MgB_2$ film grown on (110)YSZ substrate). In contrast, black curves refer to high-resistance path (current flowing in the $R_H$ direction in figure 2), to which should correspond a mixing of in-plane $\rho_{ab}$ and out-of-plane $\rho_c$ resistivities.

with no sign of a sudden increase of the resistance just before the transition, characteristic of non-homogeneous superconductors [14], supporting the high uniformity of the samples. In order to correlate the difference of the resistance path with the morphological properties of the $MgB_2$ samples, we focus our attention on the effect of film thickness on both structural and transport properties. Detailed structural characterization of $MgB_2$ films grown on (110)YSZ substrates has been extensively investigated [6]. Here we report results regarding $MgB_2$ films grown on (110)YSZ substrates, with different thicknesses. Transport properties of 600, 1300, 1500 and 3000 Å thick films are shown in figure 5. As for the previous resistance data, the two in-plane VDP configuration measurements are reported.

It is worth underlining that the value of the measured resistance $R_m$ is given by the $V_m/I_0$ ratio, where $V_m$ is the voltage drop at two near corners of the sample and $I_0$ is the bias-current value applied to the other two near corners of the sample [13]. The data clearly show that for thinner $MgB_2$ films the ratio of the two resistances in the VDP configuration is higher. This ratio is measured to be about 30 in the thinnest sample (600 Å thick) at room temperature, then decreases as the thickness of the samples increases. Eventually, in the case of the thick films (3000 Å thick), the anisotropy in the resistance paths disappears, in agreement with AFM images that show randomly in-plane oriented $MgB_2$ grains for this value of thickness.

## 4. Discussion

Transport properties of tilted $c$-axis $MgB_2$ films can be described in terms of inequivalent resistive paths, due to the different values of the out-of-plane $\rho_c$ and in-plane $\rho_{ab}$ resistivities and the specific morphological arrangement of $ab$ planes with respect to the current flow directions. According to the schematic of the $MgB_2$ tilted films shown in figure 2, in the low-resistance configuration the current flows along the Mg/B $ab$ planes: however, in the high-resistance configuration the current flows through different planes, mixing the $ab$-plane $\rho_{ab}$ and the $c$-axis $\rho_c$ contributions to the total resistivity. According to this scheme, in the thinnest $MgB_2$ films grown on (110)YSZ (in which the randomly aligned growth of tilted $MgB_2$ grains is minimized), the resistivity along the high-resistance path could be written as a linear combination of the $\rho_{ab}$ in-plane and $\rho_c$ out-of-plane resistivity. Even though a precise measurement of the $\rho_c$ value demands a controlled geometry for the resistive path, nevertheless it is still possible to estimate it by simple circuitry considerations. Let us consider the schematic of the VDP configurations as the ensemble of four resistances (figure 6), characterized by the two values $R_m^{\mathrm{High}}$ and $R_m^{\mathrm{Low}}$, corresponding to high-resistance and low-resistance paths, respectively.

It can be calculated that

$$V_m^{\mathrm{High}} = I_0 \frac{R_H}{2(R_L + R_H)} R_H \qquad (1)$$

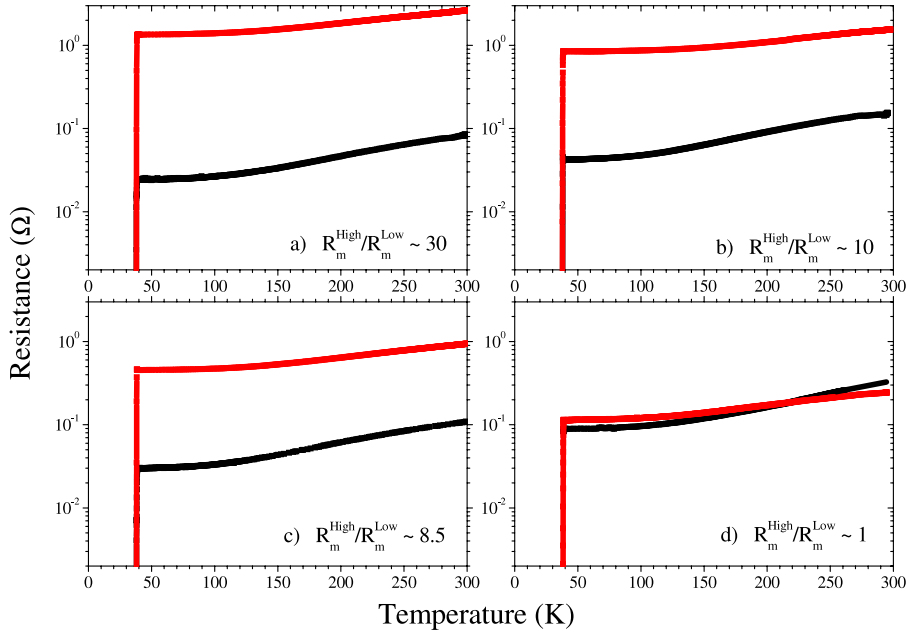


**Figure 5.** Resistance versus temperature behavior for a set of four $MgB_2$ films grown on (110)YSZ substrates, with different thickness: (a) 600 Å, (b) 1300 Å, (c) 1500 Å and (d) 3000 Å thick. As for previous data in figure 4, red and black curves refer to high-resistance ($R_H$) and low-resistance ($R_L$) paths for the two VDP configurations. For all the sample, the $R_m^{High}/R_m^{Low}$ ratio, measured at room temperature, is also reported.

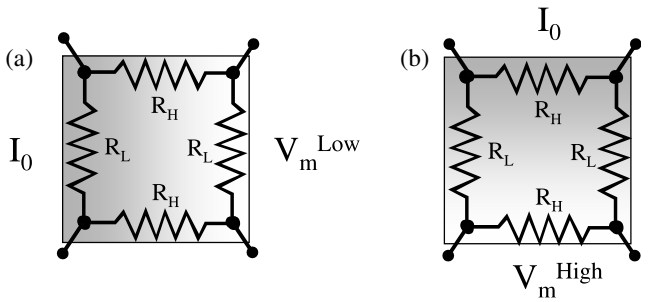


**Figure 6.** Sketch of the current/voltage geometry and corresponding equivalent circuitries for the two Van der Pauw configurations.

$$V_m^{Low} = I_0 \frac{R_L}{2(R_L + R_H)} R_L \qquad (2)$$

where $V_m^{High}$ and $V_m^{Low}$ are the voltage drops measured in the two VDP high-resistance and low-resistance configurations, respectively, and $I_0$ is the bias current. It can be derived that

$$\frac{R_m^{High}}{R_m^{Low}} = \frac{V_m^{High}}{V_m^{Low}} = \left(\frac{R_H}{R_L}\right)^2 \qquad (3)$$

where $R_m^{High}$ and $R_m^{Low}$ are the actual measured resistance values in the two VDP high-resistance and low-resistance configurations. Based on such a simple calculation it is straightforward to derive the $\rho_c/\rho_{ab}$ anisotropic ratio. Indeed, because of the square geometry of the sample, the ratio of the resistivity values along the high-resistance path ($\rho_H$) and the low-resistance path ($\rho_L$) is given by $R_H/R_L = \rho_H/\rho_L$. For the thinnest $MgB_2$ films (600 Å thick) grown on (110)YSZ, $R_m^{High}/R_m^{Low} \sim 30$, thus consequently, from equation (3), $R_H/R_L = \rho_H/\rho_L \sim 5.4$. Since the major contribution to $\rho_H$ comes from $\rho_c$, it could be estimated that $\rho_c \sim 5.4\rho_{ab}$.

An important point is the temperature at which the $R_m^{High}/R_m^{Low}$ ratio should be calculated. As a matter of fact, $MgB_2$ thin film resistivity has been shown to be strongly dependent on experimental factors, such as the film thickness, grain size and so on. It could be argued that such a ratio should be calculated at very low temperature, just above the superconducting transition, where resistivity approaches its residual value. However, $MgB_2$ residual resistivity $\rho_0$ have shown a strong dependence on the film thickness [11], ranging from 1.4 to 0.1 $\mu\Omega$ cm as the film thickness increases. Moreover, additional scattering mechanisms could arise from the peculiar morphology of the $MgB_2$ films. As shown by both SEM and AFM micrographs, in very thin films, the grains are rectangularly shaped (200 × 60 $nm^2$), thus resulting in a larger number of boundaries along the $R_m^{High}$ paths. As a consequence, the different connectivity among the $MgB_2$ grains along the two in-plane crystallographic directions could affect the different $R_m^{High}$ and $R_m^{Low}$ values. In this respect, an alternative method could consist of using the quantity $\Delta\rho \equiv \rho_{300\,K} - \rho_0$, which is a more general parameter to describe transport properties in $MgB_2$ [11, 16] and it appears to be independent of extrinsic effects (such as the film thickness, grain size and connectivity). If we use the $\Delta\rho$, by considering $\rho_0 = \rho_{40\,K}$, we obtain $\Delta R_m^{High}/\Delta R_m^{Low} \sim 21.6$, thus consequently $\rho_c \sim 4.6\rho_{ab}$. It is worth mentioning that Van der Pauw's theorem for measuring specific resistivity has been recently extended to anisotropic media [17], making possible a more accurate evaluation of the in-plane anisotropic resistivities, albeit by the determination of the conductivity tensor. Nevertheless, although unpatterned samples would not

provide a precise measurement of the $\rho_c/\rho_{ab}$ resistivity ratio, and our estimation is based on a very simple circuitry model, the value of 4.6 is quite similar to that reported in the literature for $MgB_2$ single crystals [9].

## 5. Conclusions

$MgB_2$ thin films with tilted *c*-axis growth mode can be achieved by HPCVD using suitable substrates. We have grown $MgB_2$ films on YSZ and MgO substrates and we found that, by changing the specific orientation of the substrate, the tilting angle, the tilting angle between the *c* axis of the $MgB_2$ film and the normal to the substrate's surface can be varied. A sizable anisotropy of the in-plane transport properties has been measured in *c*-axis tilted $MgB_2$ thin films. Such an anisotropy depends on the specific choice of the substrate and its orientation and on the film thickness. In particular, it decreases as the thickness of the film increases. In very thin films, in-plane resistance measurements can provide the opportunity to estimate the in-plane anisotropic resistivities ratio $\rho_c/\rho_{ab}$. Though in principle more accurate determinations are possible, by using a very simple and effective concentrated constant circuitry model, we could obtain a rough estimation of the anisotropy ratio $\rho_c/\rho_{ab} \sim 4.6$–5.4. All these findings encourage studies of the transport properties in tilted $MgB_2$ films (for instance, by changing the substrate and its crystallographic orientation, thus varying the $MgB_2$ film tilting angle), in particular as possible alternative methods to measure the in-plane $\rho_{ab}$ and the out-of-plane $\rho_c$ resistivities.

## Acknowledgments

PO's research activity at The Pennsylvania State University was partially supported by CNR under the project Short Term Mobility. The work at Penn State is supported in part by ONR under grant N00014-00-1-0294 (for X X Xi) and DOE under grant DE-FG02-08ER46531 (for Q Li). RC's research activity has received funding from the European Community's Seventh Framework Programme 2007–2011 under NFFA Grant Agreement no. 212348. The work at Argonne National Laboratory was supported by UChicago Argonne, LLC, Operator of Argonne National Laboratory ('Argonne'). Argonne, a US Department of Energy Office of Science laboratory, is operated under contract no. DE-AC02-06CH11357. The research activity of some of the authors (MP, PO, RV, RD) was partially supported by the Italian Foreign Affairs Ministry (MAE)—General Direction for Cultural Promotion. Valuable and fruitful scientific discussions with C Ferdeghini are acknowledged.

## References

[1] Xi X X 2009 *Supercond. Sci. Technol.* **22** 043001
[2] Putti M, Vaglio R and Rowell J M 2008 *Supercond. Sci. Technol.* **21** 043001
[3] Di Capua R, Aebersold H U, Ferdeghini C, Ferrando V, Orgiani P, Putti M, Salluzzo M, Vaglio R and Xi X X 2007 *Phys. Rev.* B **75** 014515
[4] Cui Y, Chen K, Li Q, Xi X X and Rowell J M 2006 *Appl. Phys. Lett.* **89** 202513
[5] Chen K, Cui Y, Li Q, Zhuang C G, Liu Z-K and Xi X X 2008 *Appl. Phys. Lett.* **93** 012502
[6] Iavarone M, Karapetrov G, Menzel A, Komanicky V, You H, Kwok W K, Orgiani P, Ferrando V and Xi X X 2005 *Appl. Phys. Lett.* **87** 242506
[7] Ferdeghini C *et al* 2002 *Physica* C **378–381** 56
[8] Cubitta R *et al* 2006 *J. Phys. Chem. Solids* **7** 493
[9] Eltsev Yu, Nakao K, Lee S, Masui T, Chikumoto N, Tajima S, Koshizuka N and Murakami M 2002 *Phys. Rev.* B **66** 180504R
[10] Zhuang C *et al* 2009 *Supercond. Sci. Technol.* **22** 025002
[11] Pogrebnyakov A V, Redwing J M, Jones J E, Xi X X, Xu S Y, Li Q, Vaithyanathan V and Schlom D G 2003 *Appl. Phys. Lett.* **82** 4319
[12] Cui Y, Jones J E, Beckley A, Donovan R, Lishego D, Maertz E, Pogrebnyakov A V, Orgiani P, Redwing J M and Xi X X 2005 *IEEE Trans. Appl. Phys.* **15** 224
[13] Van der Pauw L J 1958 *Phil. Technol. Rev.* **20** 220
[14] Vaglio R, Attanasio C, Maritato L and Ruosi A 1993 *Phys. Rev.* B **47** 15302
[15] Orgiani P, Petrov A Yu, Adamo C, Aruta C, Barone C, De Luca G M, Galdi A, Polichetti M, Zola D and Maritato L 2006 *Phys. Rev.* B **74** 134419
[16] Rowell J, Xu S Y, Zeng X H, Pogrebnyakov A V, Li Q, Xi X X, Redwing J M, Tian W and Pan X Q 2003 *Appl. Phys. Lett.* **83** 102
[17] Kleiza J, Sapagovas M and Kleiza V 2007 *Informatica* **18** 253